PAPER

Check for updates

Salting out and nitrogen effects on cloud-nucleating ability of amino acid aerosol mixtures †

Nahin Ferdousi-Rokib, [ID] [a] Kotiba A. Malek, [ID] [a] Kanishk Gohil, [ID] ‡[a] Kiran R. Pitta, [ID] [b] Dabrina D Dutcher, [ID] [cd] Timothy M. Raymond, [ID] [c] Miriam Arak Freedman [ID] [be] and Akua A. Asa-Awuku [ID] *[a]

Atmospheric aerosols exist as complex mixtures containing three or more compounds. Ternary aerosol mixtures composed of organic/organic/inorganic can undergo liquid–liquid phase separation (LLPS) under supersaturated conditions, affecting phase morphology and water uptake propensity. Phase separation and water uptake in ternary systems has previously been parameterized by oxygen to carbon (O : C) ratio; however, nitrogen containing organics, such as amino acid aerosols, also exist within complex mixtures. Yet, amino acid mixture CCN activity is poorly understood. In this study, we study the supersaturated hygroscopicity of three systems of internal mixtures containing ammonium sulfate (AS), 2-methylglutaric acid (2-MGA), and an amino acid. The three systems are AS/2-MGA/proline (Pro), AS/2-MGA/valine (Val), and AS/2-MGA/leucine (Leu). The amino acids are similar in O : C ratios but vary in solubility. Water-uptake, across a range of aerosol compositions in the ternary space, is measured using a cloud condensation nuclei counter (CCNC) from 0.4 to 1.7% supersaturation (SS). The single hygroscopicity parameter, κ, was calculated from CCNC measurements. All three systems exhibit two regions; one of these regions is phase separated mixtures when the composition is dominated by AS and 2-MGA; 2-MGA partitions to the droplet surface due to its surface-active nature and has a negligible contribution to water uptake. The second region is a homogeneous aerosol mixture, where all three compounds contribute to hygroscopicity. However, well mixed aerosol hygroscopicity is dependent on the solubility of the amino acid. Mixed Pro aerosols are the most hygroscopic while Leu aerosols are the least hygroscopic. Theoretical κ values were calculated using established models, including traditional κ-Köhler, O : C solubility and O : C-LLPS models. To account for the possible influence of polar N–C bonds on solubility and water uptake, the X : C parameterization is introduced through the X : C solubility and X : C-LLPS models; X : C is obtained from the ratio of oxygen and nitrogen to carbon. The study demonstrates competing organic–inorganic interactions driven by salting out effects in the presence of AS. Traditional methods cannot further encapsulate the non-ideal thermodynamic interactions within nitrogen-containing organic aerosol mixtures thus predictions of LLPS and hygroscopicity in nitrogen containing ternary systems should incorporate surface activity, O–C, N–C bonds, and salting out effects.

Environmental significance

A significant population of aerosols within our atmosphere exist as complex mixtures containing both organic and inorganic mixtures. Organic/inorganic aerosol mixtures may also include the presence of nitrogen containing aerosols, such as amino acids. As a result, they may present varied mixing states that can affect current projections of aerosol-cloud interactions. Thus, it is critical to understand complex amino acid aerosol mixtures' ability to become cloud condensation nuclei in order to better predict their effect on our global radiative forcing projections. In this study, the water uptake of three amino acids, ʟ-leucine, ʟ-valine, and ʟ-proline, as well as their mixtures with 2-methylglutaric acid and ammonium sulfate were investigated under supersaturated conditions. Our study shows that hygroscopicity of amino acids and their mixtures are dependent on amino acid structure and competing salting out effects due to the presence of AS. Our results demonstrate that several factors, including the presence of nitrogen and surface-active compounds, can influence droplet phase separation and aerosol water uptake ability. We further show that these effects can be parameterized to better predict hygroscopicity. Thus, physicochemical properties such as amino acid structure, the presence of nitrogen, surface activity, morphology and salting out effects must be accounted for when predicting amino acid mixture water uptake. By considering these parameters, we can better predict the effect or aerosol mixtures on our global climate.

[a]Department of Chemical and Biomolecular Engineering, University of Maryland, College Park, MD 20742, USA. E-mail: asaawuku@umd.edu

[b]Department of Chemistry, Pennsylvania State University, University Park, PA 16802, USA

[c]Department of Chemical Engineering, Bucknell University, Lewisburg, PA 17837, USA

[d]Department of Chemistry, Bucknell University, Lewisburg, PA 17837, USA

[e]Department of Meteorology and Atmospheric Science, Pennsylvania State University, University Park, PA 16802, USA

† Electronic supplementary information (ESI) available. See DOI: https://doi.org/10.1039/d4ea00128a

‡ Present address: Center for Atmospheric Particle Studies, and the Department of Chemical Engineering, Carnegie Mellon University, Pittsburgh, PA.

© 2025 The Author(s). Published by the Royal Society of Chemistry

Environ. Sci.: Atmos., 2025, 5, 485–501 | 485

1. Introduction

Atmospheric aerosols are solid or liquid particles suspended in the air and can modify cloud properties. For example, an increase in aerosol particle concentration can increase cloud lifetime and reflectivity.[1–3] Aerosol ability to form clouds, referred to as aerosol-cloud interactions, results in an overall cooling effect on our climate. Cloud formation and lifetime are driven by an aerosol's ability to uptake water, or hygroscopicity, under supersaturated (RH > 100%) conditions.[4] In particular, aerosols exposed to supersaturated water vapor in the atmosphere presents a surface for water to condense onto; the composition of the aerosols present can influence cloud formation.[4,5] However, cooling effects and subsequent radiative forcing projections from aerosol–cloud interactions present a large degree of uncertainty.[1–3] Uncertainty in aerosol–cloud radiative forcing models is attributed to the complexity of aerosol particle size and chemical composition affecting water uptake ability.[6–8]

Traditionally, droplet activation under supersaturated conditions and CCN activity of aerosols are predicted using Köhler theory.[5] In particular, several previous studies have estimated supersaturated hygroscopicity assuming all aerosol solute components are dissolved within a well-mixed, aqueous phase.[9–14] Thus, water uptake of aerosols and its mixtures can be parameterized by κ-Köhler theory.[15] Traditional κ-Köhler theory predicts water uptake by assuming all compounds instantaneously dissolve into the droplet bulk and contribute to hygroscopicity.[15] For aerosol mixtures, κ is based on the equal volume fraction contribution of individual solutes and is calculated by the Zdanovskii–Stokes–Robinson (ZSR) mixing rule.[15] The assumption of full dissolution in supersaturated aerosol droplets is challenged by the presence of partially water-soluble and insoluble compounds. Previous studies have described the effect of a solubility distribution in the bulk; in particular, studies have shown that in the presence of partially water soluble to insoluble compounds, κ-hygroscopicity is overpredicted.[15–26] Compounds with a solubility of 0.1–100 g L^{-1} can affect water uptake and CCN activity.[16,18] κ-Köhler theory can be modified by accounting for compound solubility and fraction of solute dissolved in the bulk.[16,27] If the compound is known, water solubility values can be directly applied to hygroscopicity calculations.[16,28] However, atmospheric organic aerosol composition is often unknown; readily available data from field studies provides elemental composition of organic aerosols including number of oxygen (O), carbon (C), and hydrogen (H) atoms.[29–31] Water solubility is driven by polarity and the presence of O–C bonds can contribute to compound solubility. To extend hygroscopicity models to unknown organic aerosols and field measurements, solubility can be parameterized using oxygen to carbon (O : C) ratio; limited solubility range of 0.1–100 g L^{-1} corresponds to an O : C range of 0.2–0.7.[17,25,27,32]

Parameterizations of solubility have been dependent on the presence of O–C bonds in compounds due to their polarity. However, organic aerosols may be composed of compounds containing elements other than O, C, and H; organics may also contain nitrogen (N) and N–C bonds. N–C bonds are also considered highly polar due to nitrogen's strong electronegativity. Nitrogen containing compounds are also present within our atmosphere; in this study, we focus on amino acids. Amino acids are composed of a carboxylic acid group and amino group; additionally, they are known as the building block of proteins and a source of nitrogen for organisms such as phytoplankton and bacteria.[33,34] Previous field studies have detected the presence of amino acids; furthermore, amino acids can act as ice nucleating particles (INPs) and CCN.[35–37] A study performed in Central Europe found amino acids composed up to 5% of atmospheric particulate matter within the region.[38] Similarly, a study in Beijing, China measured a total concentration of 1.86 ± 1.29 µg m^{-3} during the 2014 Asia-Pacific Economic Cooperation (APEC) summit.[35] However, amino acids are primarily found in sea spray aerosols (SSA).[39,40] Ocean bubble bursting emits SSA into the atmosphere; as a result, 11–18% of dissolved organics within submicron SSA being composed of free amino acids.[39] Previous studies have examined the water-uptake ability of amino acids as well as amino acid/AS mixtures under subsaturated (<100% RH) conditions; limited studies have evaluated amino acid hygroscopicity under supersaturated (>100% RH) conditions.[37,41–44] In subsaturated conditions, the deliquescence and morphology of amino acid/AS aerosol mixtures was dependent on the solubility of the amino acid; amino acid aerosols were found to affect the phase state of ammonium sulfate and create a liquid state when the amino acid was sparingly soluble.[44] Similarly, a study by Kristensson et al., 2010 also found that solubility effects prevailed in water uptake behavior of pure amino acids. Thus, amino acids are efficient CCN and its intrinsic solubility can present complexity in aerosol water uptake. A few studies have focused on select amino acids (e.g., aspartic acid, serine, glutamine), however supersaturated hygroscopicity data is not readily available for many other amino acids present in aerosols.[35,37,39,40,44] For example, Leucine, Valine and Proline are three amino acids found within SSA and continental aerosol samples, yet CCN measurements are not readily available.[35,39,45] The study of amino acids and nitrogen containing organic aerosol presents an opportunity to expand our scientific understanding of complex nitrogen containing aerosol species and their subsequent water-uptake. Recent studies have highlighted the growing significance of studying organic nitrogen (ON) containing aerosols due to its abundance in the atmosphere and making up a significant portion of nitrogen present in the atmosphere.[45–52] For example, a study by Yu et al., 2024 found that 17–31% of nitrogen containing aerosols studied within several urban and rural sites in China were composed of organic nitrogen.[53] Amino acids are encapsulated in these measurements; a study by Spitzy 1990 reported amino acid aerosol concentrations of 0.47–1.13 nM m^{-3} over the Bay of Bengal.[46] Additionally, a study by Gorzelska and Galloway, 1990 identified free amino acid aerosols in the range of 0.003 to 1.63 nM m^{-3} over the North Atlantic Ocean.[47] Thus, the characterization of amino acid hygroscopicity is important in further improving CCN activity predictions and projections of aerosol-cloud interaction radiative forcing.

Furthermore, the presence of amino acids may influence the morphology of aerosol particles. Both the chemical and physical

(internal morphology) composition within inorganic/organic droplets can affect hygroscopicity predictions[54–57] Uncertainty in aerosol mixture hygroscopicity predictions is attributed to organic aerosols (OA). Primary organic aerosols (POA) have the ability to oxidize, react, age, and interact with other organic/inorganic compounds.[32,58–60] Additionally, volatile organic compounds (VOCs) present in the atmosphere can oxidize and condense onto the surface of existing aerosols present; through these reaction mechanisms, secondary organic aerosols (SOA) can be formed.[58,61] OA are represented by a range of compound classes (*e.g.*, carboxylic acids, alcohols) and have varied properties based on their composition; in particular, a distribution of solubilities are present in OA.[18,29,62,63] Furthermore, organics can result in complex phase morphology within organic/inorganic aerosol mixtures.[26,64–68] In particular, aerosol mixtures can present as an outer organic layer and inorganic core, also known as liquid–liquid phase separated (LLPS) morphology.[26,64,66–68] Chemical composition, solubility and phase morphology of organic aerosols present complexity in predictions of droplet formation and CCN activity.[26]

Amino acid mixtures with inorganic compounds may further complicate solubility effects. Inorganic compounds such as AS are able to reduce the solubility of organic compounds, known as a "salting out" effect and is attributed to the presence of LLPS salting out strength is dependent on the ions present within the salt.[65,69] The presence of salts (*e.g.*, NaCl, AS) may further enhance intrinsic properties of organics. For example, surface-active compounds (*e.g.*, 2-MGA, malonic acid) mixtures result in lowered surface tension depression; the salting out effect pushes organic out of the aqueous bulk and forms an organic monolayer on the droplet surface.[70,71] Many protein studies have also described the use of AS to precipitate out proteins containing amino acids; the presence of AS can further reduce the partial water solubility of amino acids and as a result promote phase separation.[72–75] Therefore, in mixtures of higher order (three or more compounds), there may be competing organic–inorganic interactions that affect CCN activity. To our knowledge, there are no studies that examine the CCN activity of higher order amino acid mixtures under supersaturated conditions.

Recent studies have used O : C to parameterize both limited solubility and the presence of LLPS. Studies have described the presence of partially soluble compounds promoting the presence of LLPS; in particular, compounds with fewer oxygen atoms (lower O : C ratio) are more likely to phase separate in a mixture.[13,65] LLPS within mixtures occurs when the Gibb's free energy is lower for a phase separated state as opposed to remaining in a homogeneous state.[12,26,65,76] Previous studies have predicted the presence or lack of LLPS by mixture O : C ratio.[26,67,68] For example, in mixtures containing ammonium sulfate (AS), LLPS is predicted when the mixture O : C ratio <0.56; depending on the composition mixture and properties, LLPS may exist for AS mixtures of O : C 0.56–0.8.[65,68] In studies by Ott *et al.*, 2020 and Malek *et al.*, 2023, LLPS in mixtures of 2-methylglutaric acid (2-MGA), AS, and sucrose was estimated to occur at O : C ratios <0.72 and 0.75, respectively. As more sucrose (a higher O : C compound) is added to the system and O : C becomes greater than the threshold, the phase morphology shifts from phase separated to well mixed.[26,67] Previous studies have assumed that

salting out induced LLPS does not affect CCN activity due to mixed aerosols undergoing full deliquescence occurring above 100% RH.[77] Malek *et al.*, 2023 showed that phase separation does influence supersaturated hygroscopicity and incorporating O : C LLPS threshold in a hygroscopicity model best predicts κ.[26] Instead, the less soluble organic partitions to the surface; however, the studies mentioned above do not account for phase separation within nitrogen containing mixtures, such as amino acid mixtures, and the possible influence of nitrogen on LLPS estimations.

In this study, we characterize the hygroscopicity of L-leucine (Leu), L-valine (Val), and L-proline (Pro) within ternary systems containing 2-MGA and AS. Though all three amino acids have a similar O : C ratio (Leu = 0.33, Val and Pro = 0.4), solubility is varied (Leu < Val < Pro). κ-Hygroscopicity is first experimentally determined under supersaturated conditions for pure amino acids and their mixtures. Experimental hygroscopicity values are then compared against predicted hygroscopicity calculated from traditional κ-Köhler theory. In order to assess if O : C is an effective parameterization of solubility and LLPS for nitrogen containing organics, such as amino acids, the O : C-solubility model and O : C-LLPS model from Malek *et al.* 2023,[26] are used to predict κ. To date, there have been no solubility and LLPS parameterizations that incorporate other polar bonds, such as N–C, that can have an effect on water uptake. We introduce a new parameterization, X : C, to incorporate the polarity of both O–C and N–C within the amino acid in order to estimate solubility, LLPS and κ *via* the X : C-solubility, X : C-LLPS and weighted average models. Ferdousi-Rokib *et al.*, 2024 (in review)[78] also studied 2-MGA/AS mixtures and found a surface tension depression effect due to the salting out of 2-MGA; 2-MGA is an organic compound that has the ability to partition the surface and reduce droplet surface tension, also referred to as being a surface-active organic. To account for surface activity, the Modified Monolayer Surface Coverage model is also incorporated into the O : C-LLPS, X : C-LLPS and weighted average models. We discuss each model's efficacy in predicting water uptake within the three amino acid ternary systems as well as the organic–inorganic interactions driving phase separation and CCN activity.

2. Experimental methods

2.1 Chemicals

For this study, all chemicals were purchased and used without further modifications: ammonium sulfate (AS, $(NH_4)_2SO_4$; Thermo Fisher Scientific, >99.0%), 2-methylglutaric acid (2-MGA, $C_6H_{10}O_4$; Sigma-Aldrich®, 98%), L-proline (Pro, $C_5H_9NO_2$; Sigma-Aldrich®, ≥99%), L-valine (Val, $C_5H_{11}NO_2$; Sigma-Aldrich®, ≥98%), and L-leucine (Leu, $C_6H_{13}NO_2$; Sigma-Aldrich®, ≥98%). Compound chemical properties are listed in Table S1.†

2.2 Solution preparation

Three ternary systems, the Pro system (AS, 2-MGA, and Pro), the Val system (AS, 2-MGA, and Val), and the Leu system (AS, 2-MGA, and Leu) were prepared at different weight percent compositions (Fig. S1–S3 and Tables S2–4†). For each ternary system, the three

© 2025 The Author(s). Published by the Royal Society of Chemistry

Environ. Sci.: Atmos., 2025, **5**, 485–501 | **487**

chemical compounds were weighed and dissolved in ultra purified Millipore water (18 MΩ cm). Mixtures range in O : C values (Tables S2–S4†) to include experiments where LLPS is present and where LLPS is not present. The phase transition from LLPS to well mixed (LLPS threshold) is estimated based on the O : C LLPS model from Malek *et al.*[26] The model predicts the O : C threshold to be 0.50, 0.48 and 0.43 for the Pro, Val and Leu systems, respectively. To determine the effect of LLPS on cloud condensation nuclei (CCN) activity of amino acid mixtures, supersaturated hygroscopicity measurements were performed. All CCN experiment solutions are provided in Tables S5–S7.†

2.3 Cloud condensation nuclei measurements

Hygroscopicity of pure amino acids and their respective ternary systems under supersaturated (SS) conditions (>100% RH) was estimated using a Cloud Condensation Nuclei Counter (CCNC, Droplet Measurement Technologies). The theory of the CCNC has been described in previous literature.[56,79,80] Solutions were passed through a constant output Collision Nebulizer (Atomizer, TSI 3076) to generate polydisperse aerosols. Wet aerosols were dried (<5% RH) using two silica gel dryers in series.

Dried polydisperse aerosols are passed through an electrostatic classifier (TSI 3080) in scanning mode from 8 nm to 352 nm for 135 seconds. The aerosol sample flow rate is 0.8 L min^{-1} and the aerosol to sheath flow rate is 1 : 10. The monodisperse size-selected particles were then sampled by a condensation particle counter (CPC, TSI 3776) and CCNC in parallel. The CPC and CCNC operated at 0.3 L min^{-1} and 0.5 L min^{-1}, respectively. The CPC counted the number concentration of dry particles (condensation nuclei, CN) at a selected size. The particles are then exposed to 0.42 to 1.72% SS within the CCNC and the concentration of particles activated (CCN) were measured. The experimental set up was calibrated using ammonium sulfate.[56] Calibration data and the experimental set up are provided in Table S8 and Fig. S4.†

Python-based CCN Analysis Toolkit (PyCAT 1.0) analyzed all CCNC ternary and calibration data. The open-source code is available on GitHub for public use.[81] Briefly described here, PyCAT uses the scanning mobility CCN analysis (SMCA) of Moore *et al.*, 2010 in Python;[82] the activation ratio of CCN to CN was calculated for each dry particle size using PyCAT.[83] A sigmoid was fit through the data to find the critical diameter ($D_{p,50}$) where ~50% of the dry particles form cloud droplets. A charge correction is applied in PyCAT using the multi-charge correction algorithm described in Wiedensohler 1988.[84,85] For each supersaturation, the critical diameters were found and used to calculate supersaturated single-hygroscopicity parameter, κ_{CCN}.

3. Theory

Traditionally, the water uptake of aerosol mixtures can be calculated using Köhler theory. However, Köhler theory assumes full solute dissolution and equal volume-weighted solute contributions to hygroscopicity. Previous studies have shown that hygroscopicity can be estimated for known mixtures containing partially to insoluble organic compounds.[16,18,28,86]

For known and unknown compounds, limited solubility has been parameterized by the oxygen to carbon (O : C) ratio and applied to hygroscopicity estimates.[16,17,25,26] For this study, traditional Köhler theory will be compared against the four models that account for both solubility and internal particle morphology, O : C solubility model, X : C solubility model, O : C-LLPS model and X : C-LLPS model. The theory and assumptions of each model are described in the following sections.

3.1 Traditional Köhler theory

Köhler theory describes the process of water vapor condensation on particles and droplet growth by considering aerosol physicochemical properties.[5,15] To describe droplet growth, traditional Köhler theory accounts for the Kelvin effect and Raoult (solute) effect. The Kelvin effect accounts for the increase of water vapor saturation due to the curvature of the droplet. The solute effect accounts for the decrease in vapor pressure due to the presence of a soluble substance in the solvent; the solute effects contribute to the water activity term, a_w.[4,87] For compounds fully dissolved in water, a_w can be parameterized using the single hygroscopicity parameter κ as:[15,88]

$$\frac{1}{a_w} = 1 + \kappa \frac{V_s}{V_w}, \tag{1}$$

where V_s and V_w are the volume of dry solute and water, respectively. The κ parameter describes aerosol propensity to uptake water when it is assumed that the solute instantaneously dissolves.[15]

Combining both effects, the saturation ratio, S, over the droplet and the vapor pressure can described as:

$$S = \left(1 + \kappa \frac{D_d^3}{D_w^3 - D_d^3}\right)^{-1} \exp\left(\frac{4\sigma_{s/a} M_w}{RT\rho_w D_w}\right). \tag{2}$$

where, R is the universal gas constant, T is the temperature, ρ_w is the density of water, M_w is the molecular weight of water, D_w is the wet droplet diameter and D_d is the dry particle diameter.

The κ parameter be calculated from the intrinsic properties of chemically known water-soluble aerosols as follows:[88]

$$\kappa_{int} = \frac{\nu_s \rho_s M_w}{\rho_w M_s}, \tag{3}$$

where ν_s is the van't Hoff factor, ρ_s is the density, and M_s is the molecular weight of the solute. To estimate κ for aerosols composed of more than one compound, the Zdanovskii, Stokes, and Robinson (ZSR) assumption can be applied *via* the mixing rule:[15]

$$\kappa_{ZSR} = \sum_i \varepsilon_i \kappa_i, \tag{4}$$

where ε_i is the volume fraction of the individual component, i.

κ can also be derived directly from experimental hygroscopicity measurements, such as from a CCNC. For supersaturated conditions, κ_{CCN} can be described as follows:[15]

$$\kappa_{CCN} = \frac{4\left(\frac{4\sigma_{s/a} M_w}{RT\rho_w}\right)^3}{27 D_{p,50}^3 \ln^2 SS}. \tag{5}$$

In traditional κ-Köhler theory, the volume fraction of all compounds fully contributes to overall hygroscopicity (eqn (4)). However, previous studies suggests that organic solubility distribution influences both phase morphology and aerosol hygroscopicity.[16–18] Subsequent models modify traditional κ-Köhler theory to account for both organic solubility and phase morphology.

3.2 Parameterized solubility models

In the presence of partially water-soluble (0.1–100 g L^{-1}) and effectively insoluble organic compounds, thermodynamically ideal water-interactions are complicated and not captured in traditional κ-Köhler theory.[15,18–25] For known compositions, the partial water solubility can be directly applied to κ-hygroscopicity predictions.[16,28] However, solubility limitations can be parameterized using oxygen to carbon (O : C) ratio to extend theory to unknown organic compounds.[17,27] Volume based solubility, ξ, can be parameterized by O : C ratio via eqn (6):[17]

$$\ln \zeta = 20 \left[\left(\frac{O}{C} \right)^{0.402} - 1 \right]. \tag{6}$$

Limited solubility is incorporated into κ-hygroscopicity by calculated the dissolved fraction of organic solute in the droplet, $x_{i,j}$, through the following definitions:[27]

$$x_i = \frac{(G_F{}^3 - 1)\zeta_i}{\varepsilon_i}, \tag{7}$$

$$H(x_i) = \begin{cases} x_i, & x_i < 1 \\ 1, & x_i \geq 1 \end{cases}, \tag{8}$$

where G_F is growth factor calculated from D_w/D_d and $H(x_{i,j})$ is the scaling factor based on $x_{i,j}$. The overall parameterized O : C solubility hygroscopicity, $\kappa_{O:C}$, can be defined as:

$$\kappa_{O:C} = \sum_i \varepsilon_i \kappa_i H(x_i), \tag{9}$$

where $\varepsilon_{i,j}$ and $\kappa_{i,j}$ are the volume fraction and hygroscopicity of each respective compound within the aerosol sample. All compound solubilities are listed in Table S1.† Pure Leu and Val solubilities fall within the partially soluble range as defined by Petters and Kreidenweis;[16] Pro is categorized as fully soluble.[16]

Previous studies have used O : C ratio to parameterize solubility due to the polarity of O–C bonds and its influence on water solubility.[17] However, this parameterization is mainly based on organic compounds composed of O, C and H; this does not account for organic compounds containing nitrogen (N), such as amino acids. For example, amino acids contain polar amino groups that can also influence solubility. The O : C solubility parameterization presented in eqn (6), based on the work of Kuwata et al., correlated several known organic compound O : C to ξ to find the best fit parameterization.[17] To incorporate possible nitrogen effects on solubility, a new parameterization X : C is introduced where X is defined as the number of nucleophilic atoms; here, explicitly they are oxygen and nitrogen. The X : C of a mixture is defined as:

$$X : C_{mix} = \frac{\sum\limits_k \text{moles}_k \times (X : C)_k}{\sum\limits_k \text{moles}_k}, \tag{10}$$

where k represents each individual organic compound. Volume based solubility of nitrogen containing organic compounds of commonly found amino acids in nature can be correlated to their respective X : C ratios (Table S9†);[39,45] ξ can be parameterized by X : C ratio using eqn (10):

$$\xi_{X:C} = 0.06 \ln \left(\frac{X}{C} \right) + 0.064. \tag{11}$$

The newly introduced X : C solubility parameterization can then be used in eqn (7)–(9) to obtain $\kappa_{X:C}$.

3.3 Parameterized solubility – LLPS models

Previous aerosol studies have demonstrated the influence of solubility on both water uptake and droplet phase morphology.[26,67] In particular, Ott et al., 2020 found that transitions from phase separated to well mixed aerosols can be attributed by average mixture O : C ratio; the O : C ratio where phase separation ceases to exist is considered the O : C threshold.[67] For a ternary system containing 2-MGA, AS and sucrose the experimental O : C threshold was 0.72.[67] In Malek et al., 2023,[26] liquid–liquid phase separation (LLPS) was parameterized by O : C ratio for the 2-MGA/AS/sucrose ternary system and applied to κ-hygroscopicity predictions using the O : C-LLPS model.

In the O : C-LLPS model, it is assumed the organic compound with the lowest O : C (i.e., the lowest solubility) will partition to the surface of the aqueous phase when phase separation is present; it is assumed that the most soluble organic compound is well-mixed with AS in the bulk.[26] For this study, the three amino acids have lower O : C values than 2-MGA. However, 2-MGA has surface-active properties, especially when mixed with AS.[26] In this study, 2-MGA is assumed surface-active and when LLPS is present, 2-MGA likely moves to the surface and the contribution to bulk hygroscopicity of AS and the amino acid is negligible ($\varepsilon_{2\text{-MGA}} = 0$).

The O : C-LLPS model uses bootstrap sampling method to estimate the O : C threshold of a ternary system. Briefly described here, the model simulates 100 000 possible O : C thresholds within a range to find the most probable occurrence of phase separation. The range is determined by the minimum and maximum O : C values; for the Leu system the O : C ratio range is 0.33–0.67 while for the Val and Pro systems the O : C ratio range is 0.4–0.67. At activation, the solubility of the solute depends on D_w. Wet droplet diameter is estimated by using instrument SS, $D_{p,50} = D_d$ and κ_{CCN} from eqn (5) and (2); solubility is parameterized using eqn (6). For each possible O : C threshold, $\kappa_{O:C}$ (eqn (9)) is calculated based on two conditions:

(1) O : C$_{mix}$ < O : C$_{thresh}$: only Leu/Pro/Val and AS contribute to hygroscopicity within respective systems ($\varepsilon_{2\text{-MGA}} = 0$)

(2) O : C$_{mix} \geq$ O : C$_{thresh}$: all compounds contribute to hygroscopicity

O : C thresholds are tested at random across the range. For each threshold, a set of theoretical $\kappa_{O:C}$ values are calculated; for

each set the geometric mean is calculated and is referred to as κ_{thresh}; κ_{thresh} represents the potential average κ of the ternary system based on the presence of LLPS at the tested $O:C_{thresh}$. To effectively determine the true LLPS threshold, the mean κ_{thresh} is determined as this represents the most likely phase separated ternary system and $O:C_{thresh}$. The frequency of κ_{thresh} values are plotted as a Poisson distribution, where the mean κ_{thresh} bin is determined; the Poisson distribution represents the discrete distribution of an event's frequency count when the event randomly occurs. In this study, the Poisson distribution is used to represent the frequency of a mean κ_{thresh} to occur when the $O:C_{thresh}$ is tested at random. In other words, κ_{thresh} is the most probably hygroscopicity, driven by the composition and morphology that is most favorable for interactions with water. For example, the mean κ_{thresh} of the Pro system based on the Poisson distribution was found to be ~0.39 (red line, Fig. 1A). κ_{thresh} is then plotted against their $O:C$ threshold ($O:C_{thresh}$) value and a curve fit is generated. An example of the κ_{thresh} vs. $O:C_{thresh}$ is shown for the Pro system in Fig. 1B. The curve fit and mean κ_{thresh} are used to determine its corresponding $O:C_{thresh}$ (blue lines, Fig. 1B). The corresponding $O:C$ threshold to the most frequent κ_{thresh} is considered the most probable $O:C$ threshold. The mean of the Poisson distribution indicates the most favored aerosol state where the thermodynamic limit is lowest. Using the mean $O:C_{thresh}$, $\kappa_{O:C}$ is calculated using the previous two conditions; the hygroscopicity values are referred to as $\kappa_{O:C\text{-}LLPS}$. The Poisson distribution and corresponding κ_{thresh} vs. $O:C_{thresh}$ results for the Val and Leu systems are shown in Fig. S7 and 8.†

LLPS in all three amino acid ternary systems can also be parameterized with the newly introduced $X:C$ ratio. The $X:C$-LLPS model follows the methodology described above for the $O:C$-LLPS model with the exception of solubility parameterization; eqn (11) is used to parameterize volume-based solubility. The $X:C$ bootstrap range is 0.5–0.67 for the Leu system and 0.6–0.67 for both Val and Pro systems. $X:C_{thresh}$ is calculated for each system using mean of κ_{thresh} distributions and

corresponding $X:C_{thresh}$ value, shown in Fig. S9–11.† The calculated hygroscopicity values of the $X:C$-LLPS model are $\kappa_{X:C\text{-}LLPS}$.

3.4 Predictions

Once the phase separation threshold is determined, one can predict the hygroscopicity of aerosols in ternary space. However, the influence of surface-active compounds such as 2-MGA, must be accounted for. Previous studies by Malek et al., 2023 [26] and Ferdousi-Rokib et al., 2024 (in review)[78] found that 2-MGA favors partitioning to the surface in mixtures with AS. Thus, the Monolayer Surface Coverage (MSC) model from Ferdousi-Rokib et al., 2024 (in review)[78] was incorporated to only model 2-MGA/AS binary mixtures. Several studies have observed the presence of a monolayer influencing both droplet surface tension and water uptake.[89–94] However, a previous study by Bain et al., 2023 describes how surface-active organic concentration of <100 mM can create a monolayer but droplet surface tension was reflective of more dilute organic concentrations; additionally, surface tension values can be as much as >40 mN m^{-1} higher than measured surface tension values from macroscopic solutions of the same concentration.[94] Thus, the MSC model accounts for the probability of organic at the surface under dilute conditions and estimates the average droplet surface tension, $\overline{\sigma_{s/a}}$, as:

$$\overline{\sigma_{s/a}} = (1 - \varphi)\overline{\sigma_w} + \varphi\overline{\sigma_{2\text{-}MGA}}, \tag{12}$$

where φ is modified surface coverage formation probability, $\overline{\sigma_w}$ and $\overline{\sigma_{2\text{-}MGA}}$ are average experimental surface tension values of water and 2-MGA, respectively. Hygroscopicity is calculated by categorizing mixtures into three categories: (1) full dissolution (2) probability of surface coverage formation and (3) excess dissolution of surface-active organic into the bulk. For all systems, it is assumed that total AS mass dissolves into the bulk. In category 1 ($\varphi \sim 0$), 2-MGA mass enters the bulk and hygroscopicity can be calculated using eqn (9). As $0 < \varphi < 1$, 2-MGA no longer contributes to the bulk and the remaining 2-MGA mass partitions to the surface and presents a negligible contribution
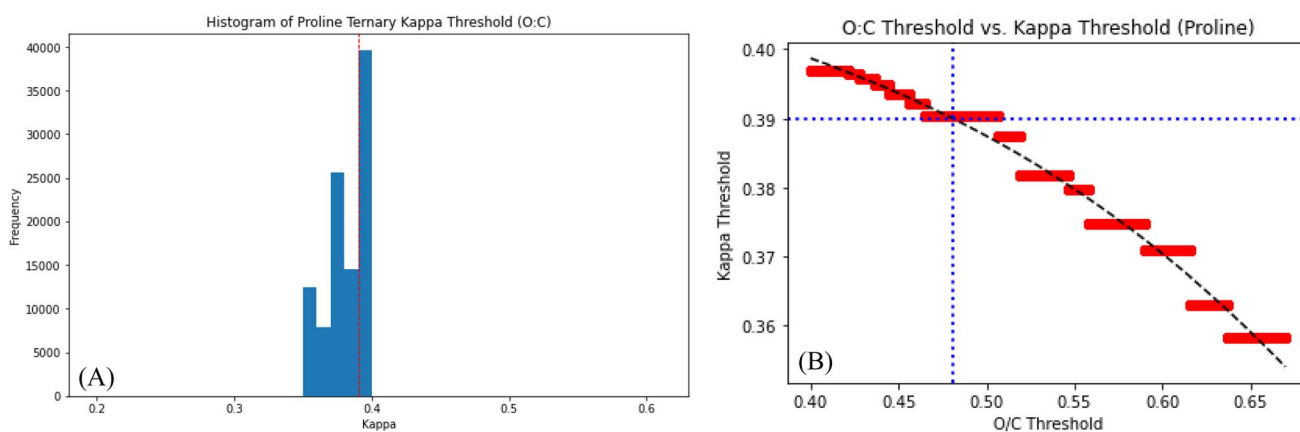

Fig. 1 $O:C$-LLPS threshold prediction results, where (A) κ_{thresh} frequency distribution after iterating 100 000 times and the most frequent bin (κ_{thresh}) shown by a red dashed line and (B) $O:C_{thresh}$ vs. κ_{thresh}, where the most frequent κ_{thresh} and its corresponding $O:C_{thresh}$ value are shown by the blue dotted lines. The corresponding $O:C_{thresh}$ value is the $O:C$ threshold of the system, where the phase separation limit is most probable and thermodynamically favorable.

to hygroscopicity. Therefore, the 2-MGA bulk mass is limited to bulk mass where φ was formally $\sim$0. Finally, the droplet surface becomes saturated ($\varphi \sim 1$) and the remaining organic mass enters the bulk. The modified monolayer formation probability φ is obtained from the dilute surface tension measurements of 2-MGA and 2-MGA/AS mixtures. For further details on the MSC model, see Ferdousi-Rokib *et al.*, 2024 (in review).[78] Hygroscopicity for 2-MGA/AS mixtures are calculated as:

$$\kappa_{2\text{-MGA/AS}} = \sum_i \varepsilon_i^b \kappa_i H(x_i). \tag{13}$$

To determine if the MSC model must be applied for amino acid/AS systems, surface tension measurements were taken for Pro, Val, and Leu. The three amino acids were found to be less surface-active than 2-MGA; for dilute concentrations, all three amino acids have a surface tension value $\sim$71 N m^{-1} (water), while 2-MGA still presents depressed surface tension (Tables S10–12 and Fig. S12–S13†). Therefore, it is assumed 2-MGA is the only organic partitioning to the surface within LLPS aerosols due to its surface activity. Surface tension measurements predictions of the ternary aerosol hygroscopicity account for varying O : C and N : C bonds that influence solubility, hygroscopicity, and phase separation.

4. Results

4.1 Experimental results of ternary systems

The water uptake of the Pro, Val and Leu ternary systems were measured under supersaturated conditions (0.42, 0.61, 0.78, 0.99, 1.21, 1.57 and 1.72% SS) using a CCNC. Each system contained mixtures of varied compositions and O : C ratios (Tables S2–S4†). Average experimental supersaturated hygroscopicity values were calculated for all mixtures across the supersaturated conditions and are reported as κ_{CCN}; the κ_{CCN} and standard deviation for all mixtures are reported in Tables S13–S15.† AS and 2-MGA κ_{CCN} were obtained from Ferdousi-Rokib *et al.*, 2024 (in review).[78] κ_{CCN} of pure Pro, Val and Leu were 0.43 ± 0.09, 0.06 ± 0.02 and 0.01 ± 0.00, respectively. κ_{CCN} values of each compound are consistent with amino acid solubility, with Pro being most soluble/hygroscopic and Leu being least soluble/hygroscopic. Val is observed to have similar water uptake as Leu although Val has the same O : C ratio as Pro; this is consistent with Val and Leu being partially soluble (88.5 and 22.4 g L^{-1}, respectively). Previous studies have emphasized the influence of solubility distribution on κ-hygroscopicity. For moderately soluble compounds (>100 g L^{-1}) such as Pro, the solute instantaneously dissolves and κ_{CCN} is driven by molar volume; for partially soluble compounds (0.1–100 g L^{-1}), such as Val and Leu, hygroscopicity is limited by the dissolved fraction of organic solute in the droplet, $x_{i,j}$, and lowers overall hygroscopicity.[16,17,27,43,81]

Limited studies have investigated amino acid hygroscopicity; for example, Raymond and Pandis investigated Leu supersaturated hygroscopicity and observed a κ_{CCN} of $\sim$0.02, similar to experimental results of this study.[15,95] However, to our knowledge, no prior studies have investigated hygroscopicity of Pro

and Val as well as ternary mixtures containing amino acids under supersaturated conditions. κ_{CCN} values were also calculated for all ternary systems and evaluated against six hygroscopicity models – traditional Köhler model, O : C solubility model, X : C solubility model, O : C-LLPS model, X : C-LLPS model and a weighted average model.

Mixtures of the three systems, Pro/2-MGA/AS, Val/2-MGA/AS and Leu/2-MGA/AS were investigated. κ_{CCN} was calculated for each ternary system *via* eqn (5) and is shown in Fig. 2 (data provided in Tables S13–S15†). All κ_{CCN} values are then presented on a contour ternary plot, where pure AS is represented on the bottom left vertex, 2-MGA on the bottom right vertex and amino acid on the top vertex. Hygroscopicity is presented as a color scale, ranging from dark purple (most hygroscopic, AS) to light yellow (least hygroscopic organic). Experimental κ_{CCN} values were used to extrapolate hygroscopicity values across the ternary contour plots (Fig. 2 and Tables S13–S15†).

For all ternary plots, κ_{CCN} range from 0.01 (pure Leucine) to 0.61 (pure AS). The overall Pro system is moderately hygroscopic, with κ_{CCN} values ranging between 0.14 (pure 2-MGA)–0.61 as seen in Fig. 2A. The ternary contour plot presents a darker purple (hygroscopic) region in the predominantly AS/2-MGA region, behaving closer to pure AS; a similar highly hygroscopic region is observed in Malek *et al.* for AS/2-MGA/sucrose ternary mixtures.[26] The AS-dominated hygroscopic region is highlighted with a dash-white line (Fig. 2A–C). The hygroscopic region is attributed to surface partitioning of 2-MGA due to surface activity as well as salting out in the presence of AS.[26] (Ferdousi-Rokib *et al.*, 2024, in review).[78]

Therefore, 2-MGA is depleted from the droplet bulk and AS drives hygroscopicity within this region; this region is considered the LLPS region. Above this region, hygroscopicity presents a direct, almost linear, correlation with organic composition, reflecting full hygroscopic contribution of all compounds; as organic mass is increasing within the mixture, κ_{CCN} is decreasing. κ_{CCN} in the region above the dashed white line are moderately hygroscopic and range from $\sim$0.1 to 0.5. This trend has previously been observed in LLPS aerosol hygroscopicity and reflects the presence of both LLPS and well mixed regions.[12,15,26]

The Val ternary system presented similar water uptake behavior to the Pro ternary system. κ_{CCN} values range from 0.06 (pure Val) to 0.61 (pure AS); pure Val is presented as yellow in the ternary contour plot, shown in Fig. 2B. The Val ternary system is also the most hygroscopic in the predominantly 2-MGA/AS (LLPS) region. The most hygroscopic region suggests that 2-MGA continues to partition to the surface and drive LLPS in both ternary systems. However, κ_{CCN} in the well-mixed region (above the dashed white-line) is lower for Val than the Pro system although Pro and Val have the same O : C ratio. This phenomenon is likely due to their solubilities, with Pro being more soluble than Val. As a result, the Val ternary system is less CCN active than the Pro system and the LLPS region is more apparent.

CCN activity of the ternary Leu system is shown in Fig. 2C. Pure Leu κ_{CCN} is represented as light yellow and experimental κ_{CCN} values ranged from 0.01 (pure Leu) to 0.61 (pure AS). The
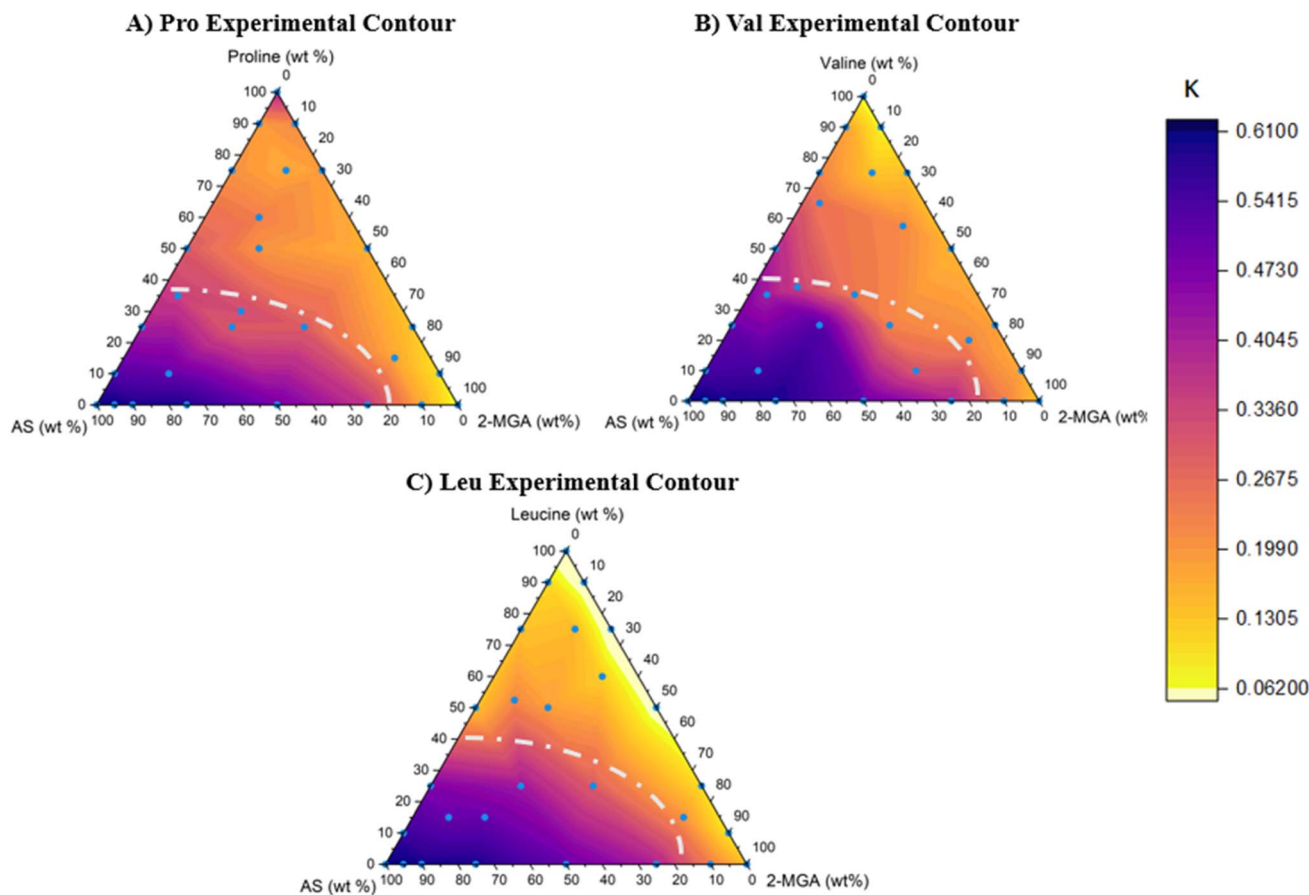
© 2025 The Author(s). Published by the Royal Society of Chemistry

Environ. Sci.: Atmos., 2025, **5**, 485–501 | 491

Fig. 2 Experimentally derived κ_{CCN} results for (A) Pro ternary system (B) Val ternary system and (C) Leu ternary system, presented on ternary contour plots. The ternary plot vertices represent pure compounds (bottom left vertex = AS, bottom right vertex = 2-MGA, and top vertex = Pro/Val/Leu). Experimental mixtures for this study are represented by blue dots in each ternary figure. κ-Hygroscopicity is represented as a color gradient where purple is most hygroscopic and light yellow is least hygroscopic. The LLPS region is outlined by a white, dashed line. LLPS is present within the purple region and above the dash line, solutes are well mixed.

Leu ternary system presented the same LLPS and hygroscopicity trends as the Pro and Val systems. However, the well-mixed region (outside of LLPS, Fig. 2C) is the least hygroscopic of all three ternary systems. The CCN activity of all systems correlate with amino acid solubility; Leu is the least water soluble and as a result, mixed Leu aerosols are less likely to uptake water than Pro and Val aerosol mixtures. All three ternary systems present similar water uptake trends but the overall κ-hygroscopicity range is dependent on pure amino acid solubility.

4.2 Modeling results and comparisons

4.2.1 Traditional κ-Köhler predictions. Experimental κ_{CCN} values for the amino acid ternary systems were compared to hygroscopicity prediction models. Traditionally, κ-hygroscopicity values are calculated using the Köhler/ZSR method, which assumes full dissolution and hygroscopic contributions of all compounds. Theoretical κ-hygroscopicity values, κ_{ZSR}, were calculated using eqn (3) and (4) and is referred to as the traditional κ-Köhler model; the model results for all systems are listed in Tables S16–18.† κ_{ZSR} was plotted on ternary contour plots and compared against the experimental contour for each ternary system (Fig. 3).

Fig. 3 shows that for all three ternary systems, the traditional κ-Köhler model (Fig. 3D–F) predicts a linear relationship between organic composition and hygroscopicity as mixtures become predominantly 2-MGA. The linear relationship does not include a phase separated hygroscopic region, as observed in experimental data (Fig. 3A–C). Previous studies have noted that traditional κ-Köhler theory is inadequate for explaining CCN activity of phase-separated or partitioned aerosols. This limitation may be due to solubility or surface activity.[26,71,89,90,92,96–99] Therefore, traditional κ-Köhler is unable to predict the surface partitioning of 2-MGA due to its assumption that all compounds fully dissolve and contribute to the bulk droplet. As a result, the traditional κ-Köhler is ineffective in predicting κ_{CCN} of all three ternary systems.

4.2.2 O : C and X : C parameterized solubility predictions. The deviation from traditional hygroscopicity predictions and experimental data has been attributed to the limited solubility distribution of organic compounds. To determine if organic solubility can effectively predict hygroscopicity of the ternary systems, we evaluate solubility for known compounds and as parameterized by O : C solubility (eqn (6)). The solubility parameterizations were then used to calculate theoretical $\kappa_{O:C}$
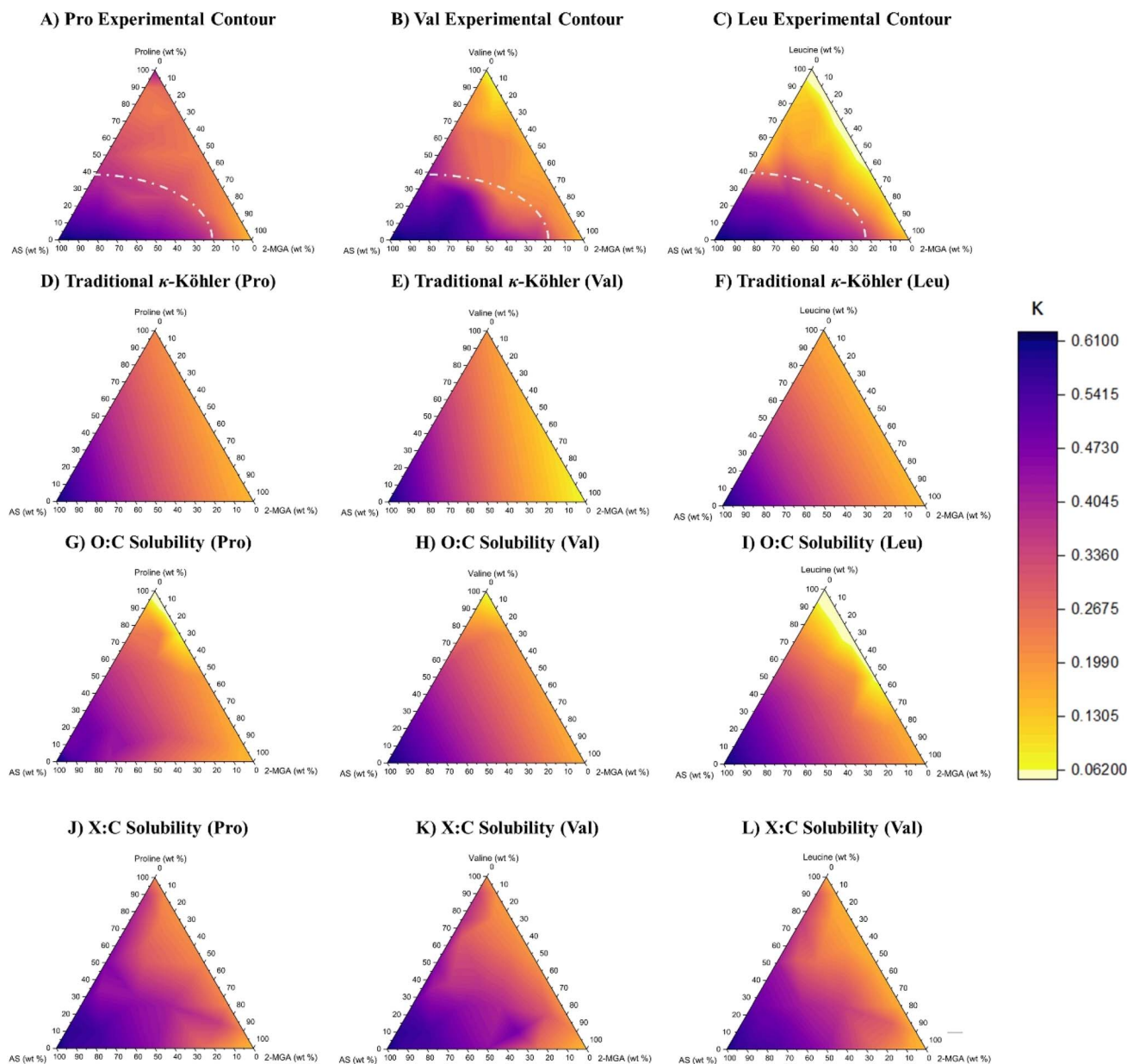
Fig. 3 Experimental κ_{CCN} results for Pro, Val and Leu (A–C) compared to κ_{ZSR} results (D–F), $\kappa_{O:C}$ results (G–I), and $\kappa_{X:C}$ results (J–L). All κ values are presented on ternary contour plots. The ternary plot vertices represent pure compounds where bottom left vertex = AS, bottom right vertex = 2-MGA, and top vertex = Pro/Val/Leu. κ-Hygroscopicity is represented as a color gradient where purple is most hygroscopic and light yellow is least hygroscopic.

using eqn (7)–(9); $\kappa_{O:C}$ was then plotted on ternary contour plots and are shown in Fig. 3G–I and Tables S16–18,† respectively. O : C solubility predicts lower κ values for all mixtures. O : C solubility predicts pure Pro and pure Val κ ~0.02; pure Leu κ is predicted to be ~0.004. Pure Leu and pure Val are better predicted by O : C solubility than pure Pro. For mixtures, O : C solubility predicts similar theoretical κ for Pro and Val mixtures; for Leu mixtures, Leu dominant mixtures (>80 wt% Leu) are predicted to be less hygroscopic. All organics and their aerosol mixtures have O : C values within 0.2–0.7. Previous studies show that the O : C solubility parameterization can be applied to organic aerosol with an O : C range of 0.2–0.7.[17,25,27] However,

pure Pro is known to be fully water-soluble (365 g L⁻¹, above the solubility limitation range of 0.1–100 g L⁻¹)[16] and the O : C solubility parametrization is inadequate for Pro and incorrectly predicts hygroscopicity. At the same time, the O : C solubility model still predicts a linear relationship between hygroscopicity and organic volume similar to traditional κ-Köhler model; the model is unable to predict the 2-MGA/AS dominated LLPS region. 2-MGA is predicted to be fully water-soluble by O : C solubility ($\kappa \sim 0.16$) but additionally partitions to the droplet surface. The LLPS region is likely dominated by surface-active 2-MGA partitioning; however, phase separation is not accounted for in the O : C solubility model.

Previous studies use O : C to parameterize solubility due to the polarity of O–C bonds driving water solubility and uptake. However, N–C bonds also present polarity that may affect solubility and water uptake properties. The X : C solubility model uses a newly introduced solubility parameterization, X : C, based on both O–C and N–C bonds (eqn (10) and (11)). $\kappa_{X:C}$ is then calculated using eqn (7)–(9) (Tables S16–18†). The model predicts overall $\kappa_{X:C}$ values greater than overall $\kappa_{O:C}$ for all three ternary systems respectively (Fig. 3J–L). This is attributed to the X : C parameterization predicting a higher solubility than the O : C parameterization due to the presence of N–C bonds. As a result, full dissolution is predicted ($H(x_{i,j}) = 1$) and the X : C solubility model presents a linear trend for all systems. Both solubility models do not estimate regions of LLPS driven hygroscopicity due to the assumption that all compounds still contribute to κ across the ternary mixture space.

4.2.3 O : C and X : C parameterized solubility & LLPS model predictions. Previous studies have observed complex morphologies in aerosol inorganic–organic and inorganic–organic–organic mixtures; these morphologies can influence water uptake.[26,64,66–68] Studies have parameterized LLPS by using O : C ratio.[26,65,67,68,100,101] To model κ_{CCN} and account for LLPS, the O : C-LLPS model, previously introduced in Malek et al., 2023[26] was used. The model predicts an O : C threshold, or O : C mixture where LLPS reaches a thermodynamic limit. Above the threshold, aerosols are considered well mixed and $\kappa_{O:C\text{-}LLPS}$ is calculated using eqn (9). Below the threshold, aerosols are considered phase separated and $\kappa_{2\text{-}MGA}$ is set to 0. The predicted O : C thresholds are 0.49, 0.51, and 0.47 for the Pro, Val, and Leu systems, respectively (Table 1). For 2-MGA/AS mixtures, the MSC model is used to calculate theoretical κ (eqn (12) and (13)). $\kappa_{O:C\text{-}LLPS}$ ternary contour plots are shown in Fig. 4D–F and Tables S16–18.†

Compared to traditional Köhler, O : C solubility, and X : C solubility models, the O : C-LLPS model successfully estimates a hygroscopic LLPS region for all three systems. The model accounts for 2-MGA partitioning due to salting out and surface activity; 2-MGA partitioning is the main driver of LLPS in the amino acid ternary systems. Therefore, calculating water uptake based on a threshold value effectively predicts phase separation in all three systems and aligns with previous studies.[26,65,67,68,100,101] However, the model is limited in predicting κ-hygroscopicity of well-mixed aerosols (above the white-dash line regions). For mixtures $\geq$ O : C$_{thresh}$, $\kappa_{O:C\text{-}LLPS} = \kappa_{O:C}$. As a result, $\kappa_{O:C\text{-}LLPS}$ underpredicts water uptake for the Pro ternary system; the model continues to underpredict Pro κ as the O : C parameterization is unable to reflect Pro solubility. The

O : C-LLPS model also underpredicts κ for a portion of the Val ternary system, shown on the Val/2-MGA axis (right side). For Val/2-MGA mixtures with >50 wt% Val, the O : C-LLPS model predicts $\kappa_{O:C\text{-}LLPS}$ of 0.02. However, κ_{CCN} reflects moderate water uptake properties and ranges from 0.06–0.16. The model best predicts κ for the Leu ternary system, especially for the Leu/2-MGA mixtures; this is represented by the light-yellow region in both Fig. 4C and F. O : C parameterization is best able to reflect the limited solubility of Leu and as a result, the O : C-LLPS model is able to predict CCN activity for both the LLPS and non-LLPS mixtures.

In addition to the O : C-LLPS model, the X : C-LLPS model was also used to predict theoretical κ to determine if both O–C and N–C bonds can effectively incorporate solubility, LLPS, and water uptake (Fig. 4G–I). The model follows a similar approach to the previous parameterized-LLPS model; now solubility and phase separation are parameterized using X : C (eqn (10) and (11)). X : C thresholds were calculated for each ternary system and are 0.65, 0.64 and 0.63 for Pro, Val and Leu, respectively (Tables S16–18†). The model is once again able to predict a hygroscopic phase separated region for predominantly 2-MGA/AS mixtures; the use of both a LLPS threshold and MSC model are effective in calculating hygroscopicity in amino acid ternary systems. For non-LLPS mixtures, $\kappa_{X:C\text{-}LLPS} = \kappa_{X:C}$. The X : C parameterization predicts higher water uptake than O : C parameterization due to both O–C and N–C bonds contributing to polarity. The X : C-LLPS model is effective in predicting water uptake for the Pro system; X : C solubility parameterization is able to predict pure Pro's higher solubility. However, the model overpredicts κ for both well mixed Val and Leu aerosol mixtures; the X : C parameterization overestimates solubility compared to O : C. The effectiveness of the O : C-LLPS and X : C-LLPS models for the different amino acid systems may be attributed to the varied influence of N–C on amino acid solubility, including in the presence of AS.[73,74,102]

4.2.4 Best fit and least χ^2 fit models. The model that best agrees with the experimental ternary system data falls within the O : C LLPS and X : C LLPS models. To assess each model's predictive ability and characterize N–C influence on water uptake, a χ^2 analysis was performed to determine the best model for each system; a smaller χ^2 value corresponds to a better fit model representative of the experimental data. χ^2 values for all ternary system models are reported in Table S19.† In addition to the previously mentioned models, an optimized weighted average of O : C-LLPS and X : C-LLPS model predictions assessed O : C and N : C contribution and determined the best fit model for all three systems. The weighted average of the two models was calculated as:

$$\kappa_{WA} = a \times \kappa_{O:C\text{-}LLPS} + b \times \kappa_{X:C\text{-}LLPS} \quad (14)$$

where coefficients a (O : C) and b (X : C) range from 0 (no contribution) to 1 (full contribution). Coefficients are calculated by simulating different values for a and b to find the least χ^2 fit for κ_{CCN} of each system; the best fit models and corresponding χ^2 values are listed in Table 2 and κ_{WA} values are listed in Tables S16–18.†

Table 1 Computationally derived thresholds for O : C-LLPS and X : C-LLPS models

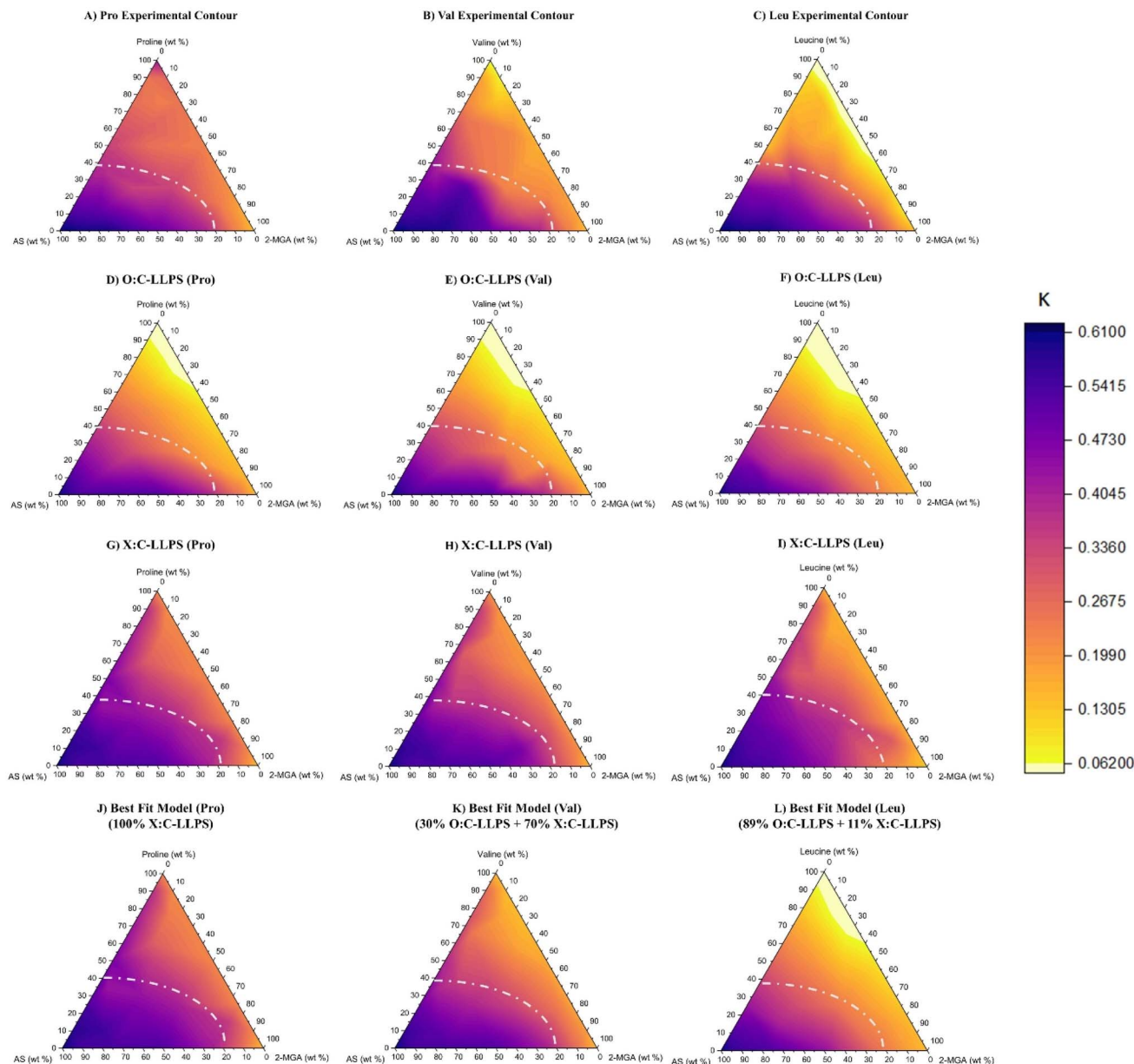| Ternary system	O : C threshold	X : C threshold
Pro/AS/2-MGA	0.49	0.65
Val/AS/2-MGA	0.51	0.64
Leu/AS/2-MGA	0.47	0.63

Fig. 4 Experimental κ_{CCN} results for Pro, Val and Leu (A–C) compared against $\kappa_{O:C\text{-}LLPS}$ results (D–F), $\kappa_{X:C\text{-}LLPS}$ results (G–I), and κ_{WA} results (J–L). All κ values are presented on ternary contour plots. The ternary plot vertices represent pure compounds where bottom left vertex = AS, bottom right vertex = 2-MGA, and top vertex = Pro/Val/Leu. κ-Hygroscopicity is represented as a color gradient where purple is most hygroscopic and light yellow is least hygroscopic.

For the Pro ternary system, the $X:C$-LLPS model was the best fit ($a = 0$ and $b = 1$). However, Val and Leu ternary systems experimental κ are best predicted by a weighted average model. The Val system is modeled by a weighted average of 0.3 $\kappa_{O:C\text{-}LLPS}$ and 0.7 $\kappa_{X:C\text{-}LLPS}$; the optimal model for the Leu system is a 0.89

$\kappa_{O:C\text{-}LLPS}$ and 0.11 $\kappa_{X:C\text{-}LLPS}$ weighted model. Amino acid best fit models are shown in Fig. 4J–L. Though all three amino acids have similar O : C ratios, O : C and N : C contribution vary between all three systems. Pro presents equal contribution of O–C and N–C bonds; Val and Leu have greater O–C influence than N–C, with Leu being most dependent on O–C. Contributions of O–C and N–C to solubility and hygroscopicity in amino acid ternary systems is correlated with the structure of each amino acid.

All three amino acids are categorized as nonpolar aliphatic; nonpolar aliphatic amino acids are defined by a carboxylic acid functional group and nonpolar, hydrophobic containing amino

Table 2 Best fit and χ^2 for amino acid ternary systems
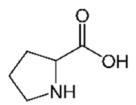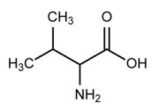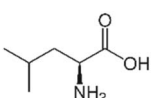
Ternary system	Best fit model	a	b	χ^2
Pro/AS/2-MGA	$X:C$-LLPS	0	1	5.23
Val/AS/2-MGA	Weighted avg.	0.30	0.70	2.85
Leu/AS/2-MGA	Weighted avg.	0.89	0.11	2.30

chain.[72,74,103] Amino acid structures are listed in Table 3. Val and Leu are open chained whereas Pro is closed chained. Previous studies investigated nonpolar aliphatic amino acid solubility in the presence of salts, like AS.[72–74] Salts such as AS and NaCl can reduce solubility ("salting out") of organics due to its ionic behavior; salt ions disrupt organic molecule hydration because of its stronger affinity to interact with water molecules.[72,74] Furthermore, salting out has been readily observed to be most effective in solutions containing salt and proteins composed of amino acids.[75] AS's anion, SO_4^{2-}, is considered an effective salting out agent.[69]

Specifically, amino acid side chain structure dictates salting out effect in the presence of salt ions. Amino acids such as Val and Leu contain a nonpolar, open side chain that is considered hydrophobic.[72,74,103] Hydrophobicity of the side chain increases with additional CH_2 groups; as a result, Leu has a more hydrophobic side chain than Val.[69,72,74] When present in an aqueous solution, salt (AS) ions disrupt the hydration of the amino acid chain containing N–C bond, reducing amino acid solubility.[72,74,103] Salting out effects are greater for Leu than Val due to the additional $-CH_2$.[72,74,102] Amino acids also contain a polar, carboxylic acid functional group containing only O–C and O–H bonds. The disruption of amino side chain (N–C) interaction with water enhances the effect of O–C in Leu and Val solubility in mixtures.[74] However, N–C still presents influence on solubility and water uptake. Val and Leu are best represented by a weighted average model with O–C given more weight, as shown by its least χ^2 fit; the contribution of N–C for the Leu system is less than the Val system ($b_{Leu} < b_{Val}$) and may be due to its longer chain enhancing salting out effects. However, Pro and its mixtures do not present salting out effects. Pro is also a nonpolar aliphatic amino acid but its side chain is cyclical (Table 3). Cyclic structures are more rigid and smaller; therefore, the compound efficiently dissolves in water and results in Pro having a higher solubility.[104] Its small structure also limits salting out effects in the presence of AS and N–C contribution is not reduced.[72] As a result, Pro is best modeled by the $X:C$-LLPS model alone; the $X:C$-LLPS model predicts equal contribution of O–C and N–C on solubility and water uptake.

Modeling each amino acid ternary system based on LLPS, solubility and salting out effects best reflects hygroscopicity. The presence of nitrogen influences both solubility and water uptake behavior; to predict water uptake, contributions of O–C and N–C must be included. Contributions of the polar bonds are dependent on the structure of the amino acid; open chain amino acids (Leu, Val) have reduced N–C effects due to their propensity to salt out in the presence of salts. Amino acids with closed side chains, such as Pro, do not salt out and can therefore be modeled by an equal contribution of O–C and N–C bonds. Therefore, chemical structure can dictate CCN activity and should be considered in predicting water uptake of complex aerosol mixtures.[105,106]

2-MGA also salts out in the presence of AS and depresses surface tension. As a result, organic surface activity influences water activity of ternary mixtures by enhancing LLPS. Malek et al.[26] correlated 2-MGA partitioning to its O : C solubility; however, in this study, 2-MGA (the more soluble organic) partitioning is due to its surface activity. Accounting for both LLPS and surface activity by using parameterized LLPS and MSC model improves water uptake prediction of amino acid ternary systems. Thus, solubility, surface activity, phase morphology and CCN activity in amino acid/2-MGA/AS systems are driven by the salting-out effects of AS. Previous studies have investigated salting out, solubility, surface activity, and phase morphology influence on CCN activity, separately.[15,16,19–25,28,89,90,93,107–109] However, studies have not accounted for all factors having a collective effect on CCN activity and subsequent κ-hygroscopicity. This study accounts for all factors having a collective effect on hygroscopicity through the incorporation of solubility parameterization and surface tension possibly driven by salting out effects in κ-hygroscopicity models.

Further work must investigate amino acids of different structures (e.g., longer/short side chain) and salts of lower order on the Hofmeister series (e.g., NaCl) to assess salting out and water uptake effects in nitrogen containing organic aerosol mixtures. Additionally, amino acids containing elements other than oxygen, nitrogen, carbon, and hydrogen exist. For example, methionine, cysteine and taurine each contain sulfur.[110] Future work should study how these additional nucleophilic compounds may affect LLPS, salting out and hygroscopicity in mixtures. Organics of stronger surfactant strength can further complicate predictions of partitioning and LLPS by enhancing solubility and salting out effects.[71,90] Therefore, studies must be performed to evaluate influence of surface activity in amino acid mixtures. In order to effectively predict κ-hygroscopicity for amino acid ternary mixtures, models must account for multiple factors (nitrogen effects on solubility, chemical structure, LLPS, surface activity), as shown by the $X:C$-LLPS and weighted average models.

5. Summary and implications

Three amino acid ternary aerosol mixtures were investigated for their water uptake properties. Mixtures were composed of ammonium sulfate, an inorganic salt, 2-methylglutaric acid, a surface-active organic, and an amino acid; amino acids

Table 3 Amino acid formula and structure

Amino acid	Formula	Structure	Side structure
Pro	$C_5H_9NO_2$		Close chain
Val	$C_5H_{11}NO_2$		Open chain
Leu	$C_6H_{13}NO_2$		Open chain

chosen for this study were proline (Pro), valine (Val), and leucine (Leu). The amino acids are similar in O : C ratios (Leu O : C = 0.33 and Pro/Val O : C = 0.4), but vary in solubility, with Pro > Val > Leu. Hygroscopicity was measured under supersaturated conditions using a CCNC. The CCNC determined the activation ratio of particles from 0.4 to 1.7% SS and an experimental κ_{CCN} was calculated. Results for all three systems showed the presence of both LLPS and well mixed aerosol across the range of mixtures in the ternary space. Mixtures with phase separated morphology are dominated by AS/2-MGA and is likely due to 2-MGA bulk-surface partitioning. For well mixed aerosol mixtures, κ_{CCN} presents a quasi-linear trend between organic composition and hygroscopicity. However, water uptake in the well mixed region parallels the solubility of the amino acid; well mixed Pro (most soluble) mixtures are the most hygroscopic while Leu (least soluble) mixtures are the least hygroscopic.

Mixtures were compared to already existing hygroscopicity models, such as traditional κ-Köhler, O : C solubility and the O : C-LLPS models. To account for the influence of nitrogen on amino acid solubility, a new parameter X : C was introduced through the X : C solubility and X : C-LLPS models. The traditional κ-Köhler, O : C solubility and X : C solubility models were unable to predict LLPS and hygroscopicity of the three amino acid ternary systems. The models predict a linear relationship between organic mass and hygroscopicity between all mixtures; this is due to the three models predicting full dissolution of 2-MGA. To account for LLPS and surface activity, the O : C-LLPS ($\kappa_{O:C-LLPS}$), X : C-LLPS ($\kappa_{X:C-LLPS}$) models, and weighted average models were used to predict theoretical κ-values. The X : C-LLPS model was identified as the best fit for the Pro ternary system. Val and Leu ternary systems were best modeled by weighted average models; the Val system had a weighted average of 0.3 $\kappa_{O:C-LLPS}$ and 0.7 $\kappa_{X:C-LLPS}$ while the Leu system was 0.89 $\kappa_{O:C-LLPS}$ and 0.11 $\kappa_{X:C-LLPS}$. The respective contributions of each model are attributed to the difference in amino acid side chain and subsequent salting out effects. Closed chain amino acids, such as Pro, are rigid and small and as a result, both O–C and N–C bonds contribute to solubility and the X : C-LLPS model performs the best for Pro. Val and Leu are open chained and salt out in the presence of AS, with salting out effects being more prominent with increased chain length (*e.g.*; Leu chain > Val chain). Therefore, O–C bonds have more influence in Val and Leu ternary systems and are best reflected by a weighted average model dependent on their side chain length.

AS/amino acid salting out are driven by amino acid chemical structure, which subsequently influences solubility and hygroscopicity, and indeed all thermodynamically driven processes. Previous studies utilize O : C parameterization for solubility, LLPS threshold, and κ-hygroscopicity predictions. However, O : C alone cannot fully encapsulate the non-ideal interactions within amino acid containing mixtures, and possibly complex nitrogen containing mixtures. The newly introduced X : C parameter is a better parameterization or can be used in addition with O : C these mixtures; this emphasizes that regardless of the amino acid structure, nitrogen still presents a degree of influence on solubility, LLPS, and hygroscopicity. Ultimately,

functional group location and properties impact droplet activation as well and must be considered. Indeed, this study aligns with previous studies, such as Suda *et al.*, 2014,[111] that have also observed the influence of functional groups on aerosol properties, including hygroscopicity. Therefore, future work including cloud parcel-based modeling studies must put more emphasis on the presence of certain functional groups within aerosol mixtures, such as carbonyl and amino groups. By accounting for functional group and nucleophiles, this study shows that we can better encapsulate nonideal behavior (*e.g.*, salting out, salting in) that can drive water uptake as well as chemical aging, aerosol surface-activity, and other possible aerosol mechanisms. However, relevant organic aerosol compounds may contain not only oxygen and nitrogen, but also sulfur. For example, methionine, an amino acid containing sulfur, has previously been attributed to lead to ultrafine particle formation within the Arctic.[112,113] Future work must therefore further investigate how other additional elements such as sulfur may present an influence on cloud microphysics.

Additionally, the ability of ammonium sulfate to drive organic partitioning demonstrates how salting out effects may further emphasize organic compound characteristics that may be traditionally overlooked when projecting aerosol-cloud interaction radiative forcing. The presence of AS enhanced solubility limitations within AS/amino dominant mixtures and enhanced surface-activity within AS/2-MGA, challenging the traditional assumption of well mixed aerosols with droplet surface tension equivalent to water. The results of this work may improve understanding of mixed nitrogen containing aerosol water uptake properties, subsequent predictions of CCN activity in larger scale models, and projections of aerosol-cloud interaction radiative forcing.

Data availability

The data supporting this article have been included as part of the ESI.†

Author contributions

NF designed, collected, analyzed CCN experimental data, produced, and analyzed theoretical models. KM contributed to design and collection of CCN experimental data. KG contributed to the development and analysis of LLPS theoretical models. All authors contributed to the writing and preparation of the manuscript.

Conflicts of interest

The authors have no competing interests to declare

References

1 Intergovernmental Panel on Climate, C., *Climate Change 2021 – the Physical Science Basis: Working Group I Contribution to the Sixth Assessment Report of the*

© 2025 The Author(s). Published by the Royal Society of Chemistry

Environ. Sci.: Atmos., 2025, **5**, 485–501 | **497**

Intergovernmental Panel on Climate Change, Cambridge University Press, Cambridge, 2023.

2 S. Twomey, The nuclei of natural cloud formation part II: The supersaturation in natural clouds and the variation of cloud droplet concentration, *Geofis. Pura Appl.*, 1959, **43**(1), 243–249.

3 S. Twomey, Pollution and the planetary albedo, *Atmos. Environ.*, 1974, **8**(12), 1251–1256.

4 J. Seinfeld and S. Pandis, *Atmospheric Chemistry and Physics: from Air Pollution to Climate Change*, 1998, p.1326.

5 H. Köhler, The nucleus in and the growth of hygroscopic droplets, *Trans. Faraday Soc.*, 1936, **32**, 1152–1161.

6 P. Saxena, *et al*, Organics alter hygroscopic behavior of atmospheric particles, *J. Geophys. Res. Atmos.*, 1995, **100**(D9), 18755–18770.

7 D. M. Murphy, D. S. Thomson and M. J. Mahoney, In Situ Measurements of Organics, Meteoritic Material, Mercury, and Other Elements in Aerosols at 5 to 19 Kilometers, *Science*, 1998, **282**(5394), 1664–1669.

8 K. A. Pratt and K. A. Prather, Aircraft measurements of vertical profiles of aerosol mixing states, *J. Geophys. Res. Atmos.*, 2010, **115**(D11), D11305.

9 A. T. Lambe, *et al.*, Laboratory studies of the chemical composition and cloud condensation nuclei (CCN) activity of secondary organic aerosol (SOA) and oxidized primary organic aerosol (OPOA), *Atmos. Chem. Phys.*, 2011, **11**(17), 8913–8928.

10 X. Tang, D. R. Cocker III and A. Asa-Awuku, Are sesquiterpenes a good source of secondary organic cloud condensation nuclei (CCN)? Revisiting β-caryophyllene CCN, *Atmos. Chem. Phys.*, 2012, **12**(18), 8377–8388.

11 L. Renbaum-Wolff, *et al.*, Observations and implications of liquid–liquid phase separation at high relative humidities in secondary organic material produced by α-pinene ozonolysis without inorganic salts, *Atmos. Chem. Phys.*, 2016, **16**(12), 7969–7979.

12 M. B. Altaf, *et al.*, Effect of Particle Morphology on Cloud Condensation Nuclei Activity, *ACS Earth Space Chem.*, 2018, **2**(6), 634–639.

13 Y. You, *et al.*, Liquid–liquid phase separation in atmospherically relevant particles consisting of organic species and inorganic salts, *Int. Rev. Phys. Chem.*, 2014, **33**(1), 43–77.

14 T. Berkemeier, *et al.*, Competition between water uptake and ice nucleation by glassy organic aerosol particles, *Atmos. Chem. Phys.*, 2014, **14**(22), 12513–12531.

15 M. D. Petters and S. M. Kreidenweis, A single parameter representation of hygroscopic growth and cloud condensation nucleus activity, *Atmos. Chem. Phys.*, 2007, **7**(8), 1961–1971.

16 M. D. Petters and S. M. Kreidenweis, A single parameter representation of hygroscopic growth and cloud condensation nucleus activity – Part 2: Including solubility, *Atmos. Chem. Phys.*, 2008, **8**(20), 6273–6279.

17 M. Kuwata, *et al.*, Classifying organic materials by oxygen-to-carbon elemental ratio to predict the activation regime of Cloud Condensation Nuclei (CCN), *Atmos. Chem. Phys.*, 2013, **13**(10), 5309–5324.

18 I. Riipinen, N. Rastak and S. N. Pandis, Connecting the solubility and CCN activation of complex organic aerosols: a theoretical study using solubility distributions, *Atmos. Chem. Phys.*, 2015, **15**(11), 6305–6322.

19 C. N. Cruz and S. N. Pandis, A study of the ability of pure secondary organic aerosol to act as cloud condensation nuclei, *Atmos. Environ.*, 1997, **31**(15), 2205–2214.

20 C. E. Corrigan and T. Novakov, Cloud condensation nucleus activity of organic compounds: a laboratory study, *Atmos. Environ.*, 1999, **33**(17), 2661–2668.

21 A. J. Prenni, *et al.*, The Effects of Low Molecular Weight Dicarboxylic Acids on Cloud Formation, *J. Phys. Chem. A*, 2001, **105**(50), 11240–11248.

22 D. A. Hegg, *et al.*, Laboratory studies of the efficiency of selected organic aerosols as CCN, *Atmos. Res.*, 2001, **58**(3), 155–166.

23 T. M. Raymond and S. N. Pandis, Cloud activation of single-component organic aerosol particles, *J. Geophys. Res. Atmos.*, 2002, **107**(D24), 1–8.

24 D. Vu, *et al.*, External and internal cloud condensation nuclei (CCN) mixtures: controlled laboratory studies of varying mixing states, *Atmos. Meas. Tech.*, 2019, **12**(8), 4277–4289.

25 P. N. Razafindrambinina, *et al.*, Hygroscopicity of internally mixed ammonium sulfate and secondary organic aerosol particles formed at low and high relative humidity, *Environ. Sci.: Atmos.*, 2022, **2**(2), 202–214.

26 K. Malek, *et al.*, Liquid–Liquid Phase Separation Can Drive Aerosol Droplet Growth in Supersaturated Regimes, *ACS Environ. Au*, 2023, **3**(6), 348–360.

27 S. Nakao, Why would apparent κ linearly change with O/C? Assessing the role of volatility, solubility, and surface activity of organic aerosols, *Aerosol Sci. Technol.*, 2017, **51**(12), 1377–1388.

28 K. Gohil and A. A. Asa-Awuku, Cloud condensation nuclei (CCN) activity analysis of low-hygroscopicity aerosols using the aerodynamic aerosol classifier (AAC), *Atmos. Meas. Tech.*, 2022, **15**(4), 1007–1019.

29 J. De Gouw and J. L. Jimenez, Organic Aerosols in the Earth's Atmosphere, *Environ. Sci. Technol.*, 2009, **43**(20), 7614–7618.

30 I. Kourtchev, *et al.*, Molecular composition of biogenic secondary organic aerosols using ultrahigh-resolution mass spectrometry: comparing laboratory and field studies, *Atmos. Chem. Phys.*, 2014, **14**(4), 2155–2167.

31 L. M. Russell, R. Bahadur and P. J. Ziemann, Identifying organic aerosol sources by comparing functional group composition in chamber and atmospheric particles, *Proc. Natl. Acad. Sci. U. S. A.*, 2011, **108**(9), 3516–3521.

32 J. L. Jimenez, *et al.*, Evolution of Organic Aerosols in the Atmosphere, *Science*, 2009, **326**(5959), 1525–1529.

33 N. J. Antia, P. J. Harrison and L. Oliveira, The role of dissolved organic nitrogen in phytoplankton nutrition, cell biology and ecology, *Phycologia*, 1991, **30**(1), 1–89.

34 K. G. McGregor and C. Anastasio, Chemistry of fog waters in California's Central Valley: 2. Photochemical transformations of amino acids and alkyl amines, *Atmos. Environ.*, 2001, **35**(6), 1091–1104.

35 S. Wang, *et al.*, Occurrence of Aerosol Proteinaceous Matter in Urban Beijing: An Investigation on Composition, Sources, and Atmospheric Processes During the "APEC Blue" Period, *Environ. Sci. Technol.*, 2019, **53**(13), 7380–7390.

36 L. F. Evans, Ice Nucleation by Amino Acids, *J. Atmos. Sci.*, 1966, **23**(6), 751–752.

37 A. Kristensson, T. Rosenørn and M. Bilde, Cloud Droplet Activation of Amino Acid Aerosol Particles, *J. Phys. Chem. A*, 2010, **114**(1), 379–386.

38 U. Pöschl, Atmospheric Aerosols: Composition, Transformation, Climate and Health Effects, *Angew. Chem., Int. Ed.*, 2005, **44**(46), 7520–7540.

39 N. Triesch, *et al.*, Sea Spray Aerosol Chamber Study on Selective Transfer and Enrichment of Free and Combined Amino Acids, *ACS Earth Space Chem.*, 2021, **5**(6), 1564–1574.

40 E. Rastelli, *et al.*, Transfer of labile organic matter and microbes from the ocean surface to the marine aerosol: an experimental approach, *Sci. Rep.*, 2017, **7**(1), 11475.

41 A. Marsh, *et al.*, Influence of organic compound functionality on aerosol hygroscopicity: dicarboxylic acids, alkyl-substituents, sugars and amino acids, *Atmos. Chem. Phys.*, 2017, **17**(9), 5583–5599.

42 M. N. Chan, *et al.*, Hygroscopicity of Water-Soluble Organic Compounds in Atmospheric Aerosols: Amino Acids and Biomass Burning Derived Organic Species, *Environ. Sci. Technol.*, 2005, **39**(6), 1555–1562.

43 S. Han, *et al.*, Hygroscopicity of organic compounds as a function of organic functionality, water solubility, molecular weight, and oxidation level, *Atmos. Chem. Phys.*, 2022, **22**(6), 3985–4004.

44 Q. Luo, *et al.*, Hygroscopicity of amino acids and their effect on the water uptake of ammonium sulfate in the mixed aerosol particles, *Sci. Total Environ.*, 2020, **734**, 139318.

45 P. J. Milne and R. G. Zika, Amino acid nitrogen in atmospheric aerosols: Occurrence, sources and photochemical modification, *J. Atmos. Chem.*, 1993, **16**(4), 361–398.

46 A. Spitzy, Amino acids in marine aerosol and rain. *Facets of Modern Biogeochemistry*, 1990, pp. 313–317.

47 K. Gorzelska and J. N. Galloway, Amine nitrogen in the atmospheric environment over the North Atlantic Ocean, *Global Biogeochem. Cycles*, 1990, **4**(3), 309–333.

48 A. Laskin, J. Laskin and S. A. Nizkorodov, Chemistry of Atmospheric Brown Carbon, *Chem. Rev.*, 2015, **115**(10), 4335–4382.

49 M. Wedyan, Bioavailability of Atmospheric Dissolved Organic Nitrogen in The Marine Aerosol over the Gulf of Aqaba, *Aust. J. Basic Appl. Sci.*, 2007, **1**(3), 208–212.

50 S. Cornell, *et al.*, Organic nitrogen in Hawaiian rain and aerosol, *J. Geophys. Res. Atmos.*, 2001, **106**(D8), 7973–7983.

51 Q. Zhang, C. Anastasio and M. Jimenez-Cruz, Water-soluble organic nitrogen in atmospheric fine particles (PM2.5) from

northern California, *J. Geophys. Res. Atmos.*, 2002, **107**(D11), 1–9.

52 K. A. Malek, *et al.*, Hygroscopicity of nitrogen-containing organic carbon compounds: o-aminophenol and p-aminophenol, *Environ. Sci.: Processes Impacts*, 2023, **25**(2), 229–240.

53 X. Yu, *et al.*, New measurements reveal a large contribution of nitrogenous molecules to ambient organic aerosol, *npj Clim. Atmos. Sci.*, 2024, **7**(1), 72.

54 D. J. Cziczo, *et al.*, Infrared spectroscopy of model tropospheric aerosols as a function of relative humidity: Observation of deliquescence and crystallization, *J. Geophys. Res. Atmos.*, 1997, **102**(D15), 18843–18850.

55 J. H. Seinfeld, Tropospheric Chemistry And Composition | Aerosols/Particles, in *Encyclopedia of Atmospheric Sciences*, ed. J. R. Holton, Academic Press, Oxford, 2003. pp. 2349–2354.

56 D. Rose, *et al.*, Calibration and measurement uncertainties of a continuous-flow cloud condensation nuclei counter (DMT-CCNC): CCN activation of ammonium sulfate and sodium chloride aerosol particles in theory and experiment, *Atmos. Chem. Phys.*, 2008, **8**(5), 1153–1179.

57 O. Laskina, *et al.*, Size Matters in the Water Uptake and Hygroscopic Growth of Atmospherically Relevant Multicomponent Aerosol Particles, *J. Phys. Chem. A*, 2015, **119**(19), 4489–4497.

58 M. Kanakidou, *et al.*, Organic aerosol and global climate modelling: a review, *Atmos. Chem. Phys.*, 2005, **5**(4), 1053–1123.

59 D. M. Murphy, *et al.*, Single-particle mass spectrometry of tropospheric aerosol particles, *J. Geophys. Res. Atmos.*, 2006, **111**(D23), D23S32.

60 Q. Zhang, *et al.*, Ubiquity and dominance of oxygenated species in organic aerosols in anthropogenically-influenced Northern Hemisphere midlatitudes, *Geophys. Res. Lett.*, 2007, **34**(13), L13801.

61 J. H. Kroll and J. H. Seinfeld, Chemistry of secondary organic aerosol: Formation and evolution of low-volatility organics in the atmosphere, *Atmos. Environ.*, 2008, **42**(16), 3593–3624.

62 M. Hallquist, *et al.*, The formation, properties and impact of secondary organic aerosol: current and emerging issues, *Atmos. Chem. Phys.*, 2009, **9**(14), 5155–5236.

63 J. H. Kroll, *et al.*, Carbon oxidation state as a metric for describing the chemistry of atmospheric organic aerosol, *Nat. Chem.*, 2011, **3**(2), 133–139.

64 A. K. Bertram, *et al.*, Predicting the relative humidities of liquid-liquid phase separation, efflorescence, and deliquescence of mixed particles of ammonium sulfate, organic material, and water using the organic-to-sulfate mass ratio of the particle and the oxygen-to-carbon elemental ratio of the organic component, *Atmos. Chem. Phys.*, 2011, **11**(21), 10995–11006.

65 M. A. Freedman, Phase separation in organic aerosol, *Chem. Soc. Rev.*, 2017, **46**(24), 7694–7705.

66 N. Riemer, *et al.*, Aerosol Mixing State: Measurements, Modeling, and Impacts, *Rev. Geophys.*, 2019, **57**(2), 187–249.

© 2025 The Author(s). Published by the Royal Society of Chemistry

Environ. Sci.: Atmos., 2025, **5**, 485–501 | **499**

67 E.-J. E. Ott, E. C. Tackman and M. A. Freedman, Effects of Sucrose on Phase Transitions of Organic/Inorganic Aerosols, *ACS Earth Space Chem.*, 2020, **4**(4), 591–601.

68 M. Song, *et al.*, Morphologies of mixed organic/inorganic/aqueous aerosol droplets, *Faraday Discuss.*, 2013, **165**, 289–316.

69 B. Kang, *et al.*, Hofmeister Series: Insights of Ion Specificity from Amphiphilic Assembly and Interface Property, *ACS Omega*, 2020, **5**(12), 6229–6239.

70 D. Topping, An analytical solution to calculate bulk mole fractions for any number of components in aerosol droplets after considering partitioning to a surface layer, *Geosci. Model Dev.*, 2010, **3**(2), 635–642.

71 N. L. Prisle, *et al.*, Surfactant partitioning in cloud droplet activation: a study of C8, C10, C12 and C14 normal fatty acid sodium salts, *Tellus B*, 2008, **60**(3), 416–431.

72 M. Aliyeva, *et al.*, Electrolyte Effects on the Amino Acid Solubility in Water: Solubilities of Glycine, l-Leucine, l-Phenylalanine, and l-Aspartic Acid in Salt Solutions of (Na+, K+, NH4+)/(Cl–, NO3–), *Ind. Eng. Chem. Res.*, 2022, **61**(16), 5620–5631.

73 L. A. Ferreira, E. A. Macedo and S. P. Pinho, Effect of KCl and Na2SO4 on the Solubility of Glycine and dl-Alanine in Water at 298.15 K, *Ind. Eng. Chem. Res.*, 2005, **44**(23), 8892–8898.

74 P. Ramasami, Solubilities of Amino Acids in Water and Aqueous Sodium Sulfate and Related Apparent Transfer Properties, *J. Chem. Eng. Data*, 2002, **47**(5), 1164–1166.

75 P. Novák and V. Havlíček, 4 – Protein Extraction and Precipitation, in *Proteomic Profiling and Analytical Chemistry*, ed. P. Ciborowski and J. Silberring, Elsevier, Boston, 2nd edn, 2016. pp. 51–62.

76 M. Song, *et al.*, Liquid-liquid phase separation and morphology of internally mixed dicarboxylic acids/ammonium sulfate/water particles, *Atmos. Chem. Phys.*, 2012, **12**(5), 2691–2712.

77 C. N. Cruz and S. N. Pandis, Deliquescence and Hygroscopic Growth of Mixed Inorganic−Organic Atmospheric Aerosol, *Environ. Sci. Technol.*, 2000, **34**(20), 4313–4319.

78 N. Ferdousi-Rokib, K. A. Malek, I. Mitchell, L. M. Fierce and A. A. Asa-Awuku, Aerosol Hygroscopicity and SurfaceActive Coverage for the Droplet Growth of Aerosol Mixtures, *Environ. Sci. Technol. Air*, 2024, in review.

79 G. C. Roberts and A. Nenes, A Continuous-Flow Streamwise Thermal-Gradient CCN Chamber for Atmospheric Measurements, *Aerosol Sci. Technol.*, 2005, **39**(3), 206–221.

80 S. Lance, *et al.*, Mapping the Operation of the DMT Continuous Flow CCN Counter, *Aerosol Sci. Technol.*, 2006, **40**(4), 242–254.

81 K. Gohil, *et al.*, Hybrid water adsorption and solubility partitioning for aerosol hygroscopicity and droplet growth, *Atmos. Chem. Phys.*, 2022, **22**(19), 12769–12787.

82 R. H. Moore, A. Nenes and J. Medina, Scanning Mobility CCN Analysis—A Method for Fast Measurements of Size-Resolved CCN Distributions and Activation Kinetics, *Aerosol Sci. Technol.*, 2010, **44**(10), 861–871.

83 K. Gohil, *kgohil27/PyCAT: v1.0 (v1.0)*, 2022.

84 N. A. Fuchs, On the stationary charge distribution on aerosol particles in a bipolar ionic atmosphere, *Geofis. Pura Appl.*, 1963, **56**(1), 185–193.

85 A. Wiedensohler, An approximation of the bipolar charge distribution for particles in the submicron size range, *J. Aerosol Sci.*, 1988, **19**, 387–389.

86 K. Gohil, *et al.*, Solubility Considerations for Cloud Condensation Nuclei (CCN) Activity Analysis of Pure and Mixed Black Carbon Species, *J. Phys. Chem. A*, 2023, **127**(17), 3873–3882.

87 H. Wex, *et al.*, The Kelvin versus the Raoult Term in the Köhler Equation, *J. Atmos. Sci.*, 2008, **65**(12), 4004–4016.

88 R. C. Sullivan, *et al.*, Effect of chemical mixing state on the hygroscopicity and cloud nucleation properties of calcium mineral dust particles, *Atmos. Chem. Phys.*, 2009, **9**(10), 3303–3316.

89 C. R. Ruehl, J. F. Davies and K. R. Wilson, An interfacial mechanism for cloud droplet formation on organic aerosols, *Science*, 2016, **351**(6280), 1447–1450.

90 J. Ovadnevaite, *et al.*, Surface tension prevails over solute effect in organic-influenced cloud droplet activation, *Nature*, 2017, **546**(7660), 637–641.

91 S. D. Forestieri, *et al.*, Establishing the impact of model surfactants on cloud condensation nuclei activity of sea spray aerosol mimics, *Atmos. Chem. Phys.*, 2018, **18**(15), 10985–11005.

92 S. Vepsäläinen, *et al.*, Comparison of six approaches to predicting droplet activation of surface active aerosol – Part 1: moderately surface active organics, *Atmos. Chem. Phys.*, 2022, **22**(4), 2669–2687.

93 J. Malila and N. L. Prisle, A Monolayer Partitioning Scheme for Droplets of Surfactant Solutions, *J. Adv. Model. Earth Syst.*, 2018, **10**(12), 3233–3251.

94 A. Bain, *et al.*, Surface-Area-to-Volume Ratio Determines Surface Tensions in Microscopic, Surfactant-Containing Droplets, *ACS Cent. Sci.*, 2023, **9**(11), 2076–2083.

95 T. M. Raymond and S. N. Pandis, Formation of cloud droplets by multicomponent organic particles, *J. Geophys. Res. Atmos.*, 2003, **108**(D15), 4469.

96 N. L. Prisle, *et al.*, Surfactants in cloud droplet activation: mixed organic-inorganic particles, *Atmos. Chem. Phys.*, 2010, **10**(12), 5663–5683.

97 T. B. Kristensen, N. L. Prisle and M. Bilde, Cloud droplet activation of mixed model HULIS and NaCl particles: Experimental results and κ-Köhler theory, *Atmos. Res.*, 2014, **137**, 167–175.

98 N. L. Prisle, A predictive thermodynamic framework of cloud droplet activation for chemically unresolved aerosol mixtures, including surface tension, non-ideality, and bulk–surface partitioning, *Atmos. Chem. Phys.*, 2021, **21**(21), 16387–16411.

99 C. R. Ruehl and K. R. Wilson, Surface Organic Monolayers Control the Hygroscopic Growth of Submicrometer Particles at High Relative Humidity, *J. Phys. Chem. A*, 2014, **118**(22), 3952–3966.

100 Y. C. Song, *et al.*, Liquid–liquid phase separation and morphologies in organic particles consisting of α-pinene and β-caryophyllene ozonolysis products and mixtures with commercially available organic compounds, *Atmos. Chem. Phys.*, 2020, **20**(19), 11263–11273.

101 S. Ham, *et al.*, Liquid–liquid phase separation in secondary organic aerosol particles produced from α-pinene ozonolysis and α-pinene photooxidation with/without ammonia, *Atmos. Chem. Phys.*, 2019, **19**(14), 9321–9331.

102 L. A. Ferreira, E. A. Macedo and S. P. Pinho, Solubility of amino acids and diglycine in aqueous–alkanol solutions, *Chem. Eng. Sci.*, 2004, **59**(15), 3117–3124.

103 C. Selvaraj, *et al.*, Chapter 3 – Macromolecular chemistry: An introduction, in *In Silico Approaches to Macromolecular Chemistry*, ed. M. E. Thomas, et al., Elsevier, 2023. pp. 71–128.

104 D. G. Peiffer, The molecular factors affecting the solubility parameter, *J. Appl. Polym. Sci.*, 1980, **25**(3), 369–380.

105 S. R. Suda, *et al.*, Influence of Functional Groups on Organic Aerosol Cloud Condensation Nucleus Activity, *Environ. Sci. Technol.*, 2014, **48**(17), 10182–10190.

106 S. S. Petters, *et al.*, Hygroscopicity of Organic Compounds as a Function of Carbon Chain Length and Carboxyl, Hydroperoxy, and Carbonyl Functional Groups, *J. Phys. Chem. A*, 2017, **121**(27), 5164–5174.

107 N. Good, *et al.*, Consistency between parameterisations of aerosol hygroscopicity and CCN activity during the RHaMBLe discovery cruise, *Atmos. Chem. Phys.*, 2010, **10**(7), 3189–3203.

108 R. Sorjamaa, *et al.*, The role of surfactants in Köhler theory reconsidered, *Atmos. Chem. Phys.*, 2004, **4**(8), 2107–2117.

109 R. Sorjamaa and A. Laaksonen, The influence of surfactant properties on critical supersaturations of cloud condensation nuclei, *J. Aerosol Sci.*, 2006, **37**(12), 1730–1736.

110 J. T. Brosnan and M. E. Brosnan, The Sulfur-Containing Amino Acids: An Overview12, *J. Nutr.*, 2006, **136**(6), 1636S–1640S.

111 S. R. Suda, M. D. Petters, G. K. Yeh, C. Strollo, A. Matsunaga, A. Faulhaber, P. J. Ziemann, A. J. Prenni, C. M. Carrico, R. C. Sullivan and S. M. Kreidenweis, Influence of Functional Groups on Organic Aerosol Cloud Condensation Nucleus Activity, *Environ. Sci. Technol.*, 2014, **48**(17), 10182–10190.

112 C. Leck and E. K. Bigg, Aerosol production over remote marine areas-A new route, *Geophys. Res. Lett.*, 1999, **26**(23), 3577–3580.

113 E. Scalabrin, *et al.*, Amino acids in Arctic aerosols, *Atmos. Chem. Phys.*, 2012, **12**(21), 10453–10463.

© 2025 The Author(s). Published by the Royal Society of Chemistry

Environ. Sci.: Atmos., 2025, **5**, 485–501 | 501